Neurobiology of Disease 76 (2015) 46–56

Contents lists available at ScienceDirect

Neurobiology of Disease

journal homepage: www.elsevier.com/locate/ynbdi

Anti-semaphorin 4D immunotherapy ameliorates neuropathology and some cognitive impairment in the YAC128 mouse model of Huntington disease

Amber L. Southwell [a], Sonia Franciosi [a], Erika B. Villanueva [a], Yuanyun Xie [a], Laurie A. Winter [b], Janaki Veeraraghavan [b], Alan Jonason [b], Boguslaw Felczak [a], Weining Zhang [a], Vlad Kovalik [a], Sabine Waltl [a], George Hall [a], Mahmoud A. Pouladi [c,d], Ernest S. Smith [b], William J. Bowers [b], Maurice Zauderer [b], Michael R. Hayden [a,*]

[a] Centre for Molecular Medicine and Therapeutics, Child and Family Research Institute, University of British Columbia, Vancouver, BC V5Z 4H4, Canada
[b] Vaccinex, Inc., Rochester, NY 14620, USA
[c] Translational Laboratory in Genetic Medicine, Agency for Science, Technology and Research, 138648, Singapore
[d] Department of Medicine, National University of Singapore, Singapore

ARTICLE INFO

Article history:
Received 11 June 2014
Revised 15 December 2014
Accepted 25 January 2015
Available online 3 February 2015

Keywords:
Semaphorin
Immunotherapy
Passive immunization
Huntington disease
Preclinical
Transgenic mice
Mouse behavior
Neuropathology

ABSTRACT

Huntington disease (HD) is an inherited, fatal neurodegenerative disease with no disease-modifying therapy currently available. In addition to characteristic motor deficits and atrophy of the caudate nucleus, signature hallmarks of HD include behavioral abnormalities, immune activation, and cortical and white matter loss. The identification and validation of novel therapeutic targets that contribute to these degenerative cellular processes may lead to new interventions that slow or even halt the course of this insidious disease. Semaphorin 4D (SEMA4D) is a transmembrane signaling molecule that modulates a variety of processes central to neuroinflammation and neurodegeneration including glial cell activation, neuronal growth cone collapse and apoptosis of neural precursors, as well as inhibition of oligodendrocyte migration, differentiation and process formation. Therefore, inhibition of SEMA4D signaling could reduce CNS inflammation, increase neuronal outgrowth and enhance oligodendrocyte maturation, which may be of therapeutic benefit in the treatment of several neurodegenerative diseases, including HD. To that end, we evaluated the preclinical therapeutic efficacy of an anti-SEMA4D monoclonal antibody, which prevents the interaction between SEMA4D and its receptors, in the YAC128 transgenic HD mouse model. Anti-SEMA4D treatment ameliorated neuropathological signatures, including striatal atrophy, cortical atrophy, and corpus callosum atrophy and prevented testicular degeneration in YAC128 mice. In parallel, a subset of behavioral symptoms was improved in anti-SEMA4D treated YAC128 mice, including reduced anxiety-like behavior and rescue of cognitive deficits. There was, however, no discernible effect on motor deficits. The preservation of brain gray and white matter and improvement in behavioral measures in YAC128 mice treated with anti-SEMA4D suggest that this approach could represent a viable therapeutic strategy for the treatment of HD. Importantly, this work provides in vivo demonstration that inhibition of pathways initiated by SEMA4D constitutes a novel approach to moderation of neurodegeneration.

Introduction

Semaphorins are a family of transmembrane proteins that influence a range of processes related to health and disease, including the development and regeneration of the central nervous (CNS) and cardiovascular systems (Hota and Buck, 2012), as well as physiologic and pathologic immune responses (Suzuki et al., 2008). In the CNS, semaphorin 4D (SEMA4D), a class IV semaphorin, is expressed on infiltrating immune cells and oligodendrocyte precursor cells and its receptors are expressed on neurons, oligodendrocytes, astrocytes and endothelial cells (Okuno et al., 2010) and unpublished observations. SEMA4D has been shown to serve as an axonal guidance molecule (Swiercz et al., 2002) as well as mediating GABAergic and glutamatergic synapse development (Paradis et al., 2007) among other activities. In the periphery, the highest expression of SEMA4D is observed on T cells and less abundantly on B cells, macrophages and dendritic cells

Abbreviations: CNS, central nervous system; DARPP-32, dopamine- and cAMP-regulated phosphoprotein; EAE, experimental autoimmune encephalomyelitis; HTT, huntingtin; HD, Huntington disease; ICV, intracerebroventricular; IP, intraperitoneal; IT, intrathecal; mAb, monoclonal antibody; mu, mutant; SEMA4D, semaphorin 4D; WT, wild-type.

* Corresponding author at: 950 W 28th Ave. Vancouver, BC V5Z 4H4, Canada.
E-mail address: mrh@cmmt.ubc.ca (M.R. Hayden).
Available online on ScienceDirect (www.sciencedirect.com).

http://dx.doi.org/10.1016/j.nbd.2015.01.002
0969-9961/

where expression is significantly upregulated upon cellular activation (Bougeret et al., 1992; Shi et al., 2000). SEMA4D has been reported to play a role in immune cell activation and migration (Suzuki et al., 2008).

The SEMA4D protein consists of a short cytoplasmic tail, transmembrane domain and extracellular Ig and Sema domains (Furuyama et al., 1996; Hall et al., 1996; Shi et al., 2000) and acts on three known receptors, Plexin-B1, Plexin-B2 and CD72 (Suzuki et al., 2008). Both membrane-associated SEMA4D as well as an extracellular soluble fragment, which results from cleavage of the protein by membrane metalloproteases between the transmembrane and Ig domains, are biologically active (Elhabazi et al., 2001; Zhu et al., 2007).

In addition to axonal guidance and synapse formation (Kuzirian et al., 2013; Raissi et al., 2013), SEMA4D has been shown to play a role in migration and differentiation of neuronal and oligodendrocyte precursor cells, CNS inflammation and neurodegeneration. For example, SEMA4D deficiency leads to increased oligodendrocyte differentiation, whereas exogenously added soluble SEMA4D inhibits oligodendrocyte differentiation (Yamaguchi et al., 2012). Interestingly, SEMA4D expression is increased in the cerebrospinal fluid of patients with human T-lymphotropic virus 1-associated myelopathy in which T cell-derived SEMA4D induces collapse of process extension of immature oligodendrocytes and death of immature neural cells, resulting in compromised remyelination of the inflamed brain (Giraudon et al., 2004). Further, SEMA4D-deficient mice are resistant to the development of experimental autoimmune encephalomyelitis (EAE) (Kumanogoh et al., 2000), and blockade of SEMA4D significantly inhibits microglial activation and neuroinflammation in EAE (Okuno et al., 2010). Similarly, SEMA4D stimulation of endothelial cells leads to production of the pro-inflammatory cytokine IL-8 (Yang et al., 2011). These observations implicate SEMA4D as playing a role in potentiating CNS inflammation and neurodegeneration and suggest that SEMA4D is a potential therapeutic target for treatment of neurodegenerative diseases.

A high affinity neutralizing antibody to SEMA4D, mAb67-2, has been described that inhibits development of EAE and promotes remyelination following chemically-induced demyelination (Smith et al., 2014). mAb67-2 is a monoclonal antibody specific for both soluble and membrane-associated SEMA4D and cross-reactive on human, primate, rat and mouse SEMA4D with comparable affinity (between 1 and 5.7 nM, as determined by surface plasmon resonance). The antibody inhibits interaction between SEMA4D and all of its known receptors, PlexinB1, PlexinB2, and CD72. In vivo delivery of mAb67-2 should block signaling cascades initiated by SEMA4D and result in reduced CNS inflammation, increased neuronal outgrowth and increased oligodendrocyte maturation and process formation. In fact, anti-SEMA4D treatment has been shown to be beneficial in multiple rodent models of EAE, leading to increased oligodendrocyte precursor cell survival, migration and maturation, remyelination, restored blood–brain barrier integrity, and improved clinical scores (Smith et al., 2014). Considering the convergent pathogenic pathways of neuroinflammatory and neurodegenerative diseases (Borjabad and Volsky, 2012; Ehrnhoefer et al., 2011; Ellwardt and Zipp, 2014; Lassmann, 2011), anti-SEMA4D treatment may have benefits in other indications, including Huntington disease (HD).

HD is an inherited, fatal neurodegenerative disease resulting from the pathogenic expansion of a polyglutamine encoding CAG tract in exon 1 of the huntingtin (*HTT*) gene to 36 or more repeats (HDCRG, 1993). HD is characterized by motor and cognitive deficits and psychiatric disturbance with death usually occurring 15–20 years after onset. There is currently no disease modifying therapy available for HD (Ross and Tabrizi, 2011). While disease onset, defined as presentation of motor deficits, typically occurs in mid-life, many features of HD present years to decades earlier, including immune activation (Bjorkqvist et al., 2008), striatal atrophy and loss of brain white matter (Tabrizi et al., 2009). Additionally, a recent study has demonstrated severely reduced turnover of cells of the neuronal and oligodendrocyte lineage within the human HD striatum (Ernst et al., 2014), indicating impairments in adult striatal neurogenesis and oligodendrogenesis. Transcriptional dysregulation is an early feature of HD, and a previous study has found that expression of SEMA4D and its major CNS receptor, Plexin-B1, are elevated in grade 0–2 HD striatum and cortex, but not cerebellum (Hodges et al., 2006), suggesting that increased SEMA4D signaling may play a role in HD pathogenesis. With the potential for anti-inflammatory effects, increased neuronal progenitor survival and process extension, and increased oligodendrocyte migration and maturation, inhibition of SEMA4D signaling through anti-SEMA4D treatment represents a novel approach to therapy for HD.

Materials and methods

Mice and treatments

Mice were maintained under a 12-h light:12-h dark cycle in a clean facility and given free access to food and water. Experiments were performed with the approval of the animal care committee of the University of British Columbia. YAC128 and wild-type (WT) littermates (Slow et al., 2003) were divided into mAb67-2 (α-Sema4D) or isotype matched mAb 2B8 (Ctrl) IgG treatment groups (35 WT ctrl, 34 WT α-Sema4D, 35 YAC128 ctrl, 36 YAC128 α-Sema4D). Mice received treatments by weekly intraperitoneal (IP) mAb injection beginning at 6 weeks of age. The majority of mice were kept until 12 months of age, but a small group (9 WT ctrl, 10 WT α-Sema4D, 10 YAC128 ctrl, 11 YAC128 α-Sema4D) was sacrificed at 6 months of age to provide interim neuropathological data. Serum was collected at 3, 6, 9, and 12 months of age by saphenous vein blood draw.

Plexin-B2 and GFAP immunohistochemistry

5-μm PFA-fixed, paraffin-embedded sections were deparaffinized using xylene baths and rehydrated with graded ethanol baths. Epitope retrieval was carried out by a 20-min boil with Target Retrieval Solution (Dako) followed by 30-min cooling. Slides were washed twice with PBS containing 0.05% Tween-20 (TPBS), and nonspecific binding was blocked by a 20-min incubation with 2.5% normal goat serum in TPBS. Following a single TPBS wash, slides were incubated for 60 min with 1:1000 rabbit anti-GFAP (1:1000, Millipore) and 3 μg/ml mouse anti-PlexinB2 (Millipore) in TPBS. Slides were then washed three times with TPBS and incubated for 30 min with Alexa 488 labeled goat anti-mouse IgM (1:400, Invitrogen) and Alexa 647 labeled donkey anti-rabbit IgG (1:400, Invitrogen) in TPBS. Slides were then washed twice with TPBS and incubated for 10 min with 1 μg/ml DAPI in TPBS, washed once with TPBS, and coverslip was mounted with Prolong Gold Antifade mounting medium (Life Technologies). Slides were imaged at 60× magnification using an Exi Aqua camera coupled to an Olympus Ix50 microscope.

SEMA4D and Plexin-B1 qRT-PCR

Twelve month old WT and YAC128 mice were killed with an overdose of avertin. Brains were removed and microdissected by region then stored in RNAlater (Ambion). Total RNA was extracted from mouse cortex or striatum with RNeasy Mini Kit or RNeasy Micro Kit (Qiagen) and treated with RNase-free DNaseI. First-strand cDNA was prepared from 1 μg (cortex) or 180 ng (striatum) of total RNA using SuperScriptIII First-Strand Synthesis System (Invitrogen). About 40 ng of cDNA was used in a final volume of 10 μl with Power SYBR Green PCR Master Mix (ABI). Comparative Ct Assay was performed using ABI 7500 Fast Real-Time PCR System under default condition. mRNA expression levels of target genes (SEMA4D S: CTCATCACTGCCCTTGGACT, SEMA4D AS: ACCCGTTGACATCCTGAAAG, Plexin-B1 S: TCCTCACGCA GAATGGTTTT, Plexin-B1 AS: AAGGTGCCTCCCTTCCTGTA) were normalized to 18S RIBO for the cortex (18S-Ribo S: GATTAAGTCCCTGCCCTTTG,

18S-Ribo AS: CAAGTTCGACCGTCTTCTCA) or UBC for the striatum (UBC S: AGCCCAGTGTTACCACCAAG, UBC AS: ACCCAAGAACAAGCACAAGG).

Serum analysis

Evaluation of α-Sema4D mAb67-2 levels in the sera of study animals was performed through the use of a qualified sandwich ELISA. The assay format consists of coating recombinant marmoset SEMA4D as a capture antigen on a microtiter plate. Serum samples were added to the plate, incubated, and unbound components removed through a wash step. Bound mAb67-2 was subsequently detected with a horseradish peroxidase-conjugated goat anti-mouse IgG1 antibody; addition of TMB (3,3′,5,5′-tetramethylbenzidine) allowed the complex to be determined colorimetrically. The concentration of mAb67-2 present in murine test samples was calculated by linear regression against a reference standard prepared in mouse serum matrix. The lower limit of quantitation of this assay was 9.3 ng/mL while the upper limit was 200 ng/mL. The minimum required dilution (MRD) for the system was 1:100.

Behavior testing

All behavior experiments were carried out during the animals' dark phase by a researcher blind to genotype and treatment. Spontaneous alternation was performed under red lighting. All other tests were performed under white lighting.

Rotarod

Two month-old mice were trained on a fixed speed rotarod (Ugo Basille) over 3 consecutive days during which motor learning was assessed as in Southwell et al. (2013). For longitudinal rotarod testing at 2-month intervals from 2 to 12 months of age, an accelerating program from 5 RPM to 40 RPM over 300 s was used. Mice received 3 trials with a 1-h inter-trial interval and the latency to the first fall was recorded. The average of the 3 testing trials was scored.

Climbing

Mice were placed at the bottom end of a closed-top wire mesh cylinder (10 × 15 cm) on the tabletop and recorded with a video camera for 5 min. The latency to begin climbing (all four feet off the tabletop), number of climbing events, and the total time spent climbing during the 5-min trial were scored. Mice were tested longitudinally at 2-month intervals from 2 to 12 months of age.

Spontaneous alternation

Four month-old mice were assessed for preference to explore the novel arm of a T-maze as described in Carroll et al. (2011a). Briefly, mice were placed at the base of the T and allowed to choose a goal arm. A barrier was then lowered to prevent exit from the goal arm during a 1-min exploration. Mice were then immediately placed at the base of the T and once again allowed to choose a goal arm. Mice that entered the previously explored goal arm were given a score of 0, while mice that entered the novel arm were given a score of 1.

Open field exploration and object learning

Anxiety during a 10-min exploration of an open field, the preference for a known object in a novel location, and the preference for a novel object were evaluated at 6 months of age as previously described in Southwell et al. (2013). Activity was recorded by a ceiling-mounted video camera and scored by Ethovision XT 7 animal tracking software (Noldus Information Technology). For open field exploration, activity was assessed by total distance traveled and mean velocity, and anxiety-like behavior was assessed by entries into and time spent in the center of the field. For object learning, the percentage of investigations to the target object (either the one in the novel location or the unfamiliar one) was computed.

Elevated plus maze

Anxiety during a 5-min exploration of an elevated plus maze was evaluated in mice aged 8 months as in Southwell et al. (2013) using a ceiling-mounted video camera and Ethovision XT 7. Distance traveled and average velocity was assessed as a measure of exploratory activity. Entries into and time spent in the open arms, in addition to head dips off the edge of the open arms, were scored as a measure of anxiety.

Porsolt forced swim test

A modified Porsolt forced swim test as in Pouladi et al. (2009) was used to assess depressive-like behaviors in mice at their final behavioral testing point (6 or 12 months). Briefly, mice were placed in individual cylinders (25 cm tall × 19 cm wide) filled with room temperature water (23–25 °C) to a depth of 15 cm for a period of 6 min. The test sessions were recorded by a ceiling-mounted video camera. Time spent swimming versus floating (immobile) in the last 5 min of the trial was scored as a measure of depressive-like behavior.

Neuropathology and immunohistochemistry

All neuropathology and quantitative immunohistochemistry was performed by researchers blind to genotype and treatment.

Tissue preparation

Mice were perfused intracardially and brains prepared as in (Southwell et al., 2013). Forebrains were then cut by cryostat into 25-μm free-floating coronal sections. Sections were stored in PBS with 0.08% sodium azide at 4 °C until immunohistochemical processing.

Immunohistochemistry

For each antigen evaluated, a series of 25-μm coronal sections spaced 200 μm apart spanning the striatum was used. Sections were then incubated for 30 min at RT in 3% H_2O_2 to deplete endogenous peroxidases, washed and incubated in primary antibody (Mouse anti-NeuN (neuronal nuclei), 1:1000, Millipore; rat anti- dopamine- and cAMP-regulated phosphoprotein (DARPP-32), 1:5000, R&D Systems) overnight at room temperature. Sections were washed and incubated with biotinylated secondary antibody (1:1000; Vector) for 2 h at room temperature. Signal was amplified using the Vectastain ABC kit, and staining was visualized using metal enhanced DAB (Thermo Scientific).

Quantitation of DARPP-32

Sections were photographed using a Zeiss Axioplan 2 microscope and Coolsnap HQ Digital CCD camera (Photometrics). The amount of DARPP-32 was determined using MetaMorph software version 6.3 (Universal Imaging Corporation). Labeling was identified and background excluded using threshold levels for all images and analyzed using "integrated morphometry". Relative levels of staining were calculated as the sum of the integrated optical density (IOD) for each image divided by the area of the region selected then multiplied by the sampling interval (8) and section thickness (25 μm)(Southwell et al., 2013). IOD was then normalized to WT Ctrl. No staining was observed in a negative control without primary antibody.

Stereological volumetric assessments

In the NeuN-stained section series, striatal, cortical and corpus callosum volumes were determined by tracing the perimeter of the desired structure in serial sections using StereoInvestigator software (Microbrightfield) and volumes determined using the Cavalieri principle. The thickness of each layer (I, II/III, IV and V/VI) in the primary motor or sensory cortex was measured using the StereoInvestigator software "measure" tool.

Statistical analysis

Longitudinal data were analyzed by 2-way analysis of variance (ANOVA) for age or training day and group and Bonferroni post-hoc analysis. Single time point data was analyzed by 2-way ANOVA for genotype and treatment or trial and Bonferroni post-hoc analysis. Results from ANOVA analysis are presented in Supplementary Table S2 and results from Bonferroni post-hoc analysis are presented on graphs. On longitudinal graphs, * represents difference from WT Ctrl group (where post-hoc comparison to WT Ctrl group is not different for YAC128 Ctrl and YAC128 α-Sema4D groups, only 1 significance marker is included). On single time point graphs, * represents difference between indicated bars, ns = not significant, * = $p < 0.05$, ** = $p < 0.01$, ***$p < 0.001$. N for each group is reported on the bars for bar graphs or in Supplementary Table S3 for line graphs.

Results

Study overview

We employed the YAC128 mouse model of HD (Slow et al., 2003) to assess the preclinical therapeutic efficacy of anti-SEMA4D immunotherapy for HD. YAC128 and WT littermates received weekly IP injections of mAb67-2 (α-Sema4D) or mAb 2B8 (Ctrl) from 6 weeks of age until 6 or 12 months of age, and were evaluated for CNS and peripheral pathology, longitudinal motor performance, psychiatric behaviors, and cognitive performance.

The SEMA4D signaling pathway in YAC128 brain

To determine if the SEMA4D signaling pathway is dysregulated in the YAC128 mouse model of HD as it is in the HD brain, we assessed the relative expression of SEMA4D and its major CNS receptor, Plexin-B1, in the striatum and cortex of 12 month-old YAC128 and WT littermates. Similar to previously reported data from HD patient brain (Hodges et al., 2006), we observed an increase in SEMA4D expression in the striatum of 12 month old YAC128 mice (Fig. 1A). While Plexin-B1 is also elevated in the human HD striatum, we observed a trend toward decreased expression in YAC128 striatum (Fig. 1C), which could be the result of compensation for increased SEMA4D expression. Additionally, while both genes are elevated in HD cortex, we observed no alterations in cortex of YAC128 mice (data not shown). These differences between YAC128 brain and human HD brain could be the result of imperfect concordance of gene expression changes between the two (Becanovic et al., 2010) or the fact that the YAC128 model is a model of early disease and many of the HD-like gene expression changes that are observed in the brains of YAC128 mice are not yet evident at 12 months of age (Kuhn et al., 2007). We next performed immunohistochemical analysis of SEMA4D and one of its major CNS receptors, Plexin-B2, in striata of 12 month old YAC128 and WT mice. Elevated Plexin-B2 receptor protein was observed on GFAP positive activated astrocytes in YAC128 brain (Fig. 1C). Combined with the observed striatal gene expression changes, these data indicate that the SEMA4D signaling pathway is disrupted in the YAC128 brain, and therefore, that the YAC128 mouse is an appropriate model system for evaluation of SEMA4D immunotherapy for HD.

Neuropathology

Similar to human HD, YAC128 mice exhibit selective and progressive loss of striatal, cortical, and white matter volumes (Carroll et al., 2011b). To assess the effect of α-Sema4D treatment on HD-like neuropathological features in YAC128 mice, the post-perfusion brains of 6- or 12-month old YAC128 mice were coronally sectioned and stained for either NeuN, a marker of all neuronal nuclei, or DARPP-32, a marker of healthy medium spiny striatal neurons. NeuN-stained sections were used to assess sub-region atrophy within the brain (Figs. 2, S1, and S2). At 6 months of age, Ctrl-treated YAC128 mice displayed expected striatal atrophy (6.4% loss), which was ameliorated by α-Sema4D treatment (3.8% loss). However, at this early time point the other neuropathological endpoints assessed revealed only trends toward genotypic differences, precluding a full assessment of the effects of anti-SEMA4D immunotherapy (Fig. S2). At 12 months of age, Ctrl-treated YAC128 mice displayed a broad range of neuropathological features, including

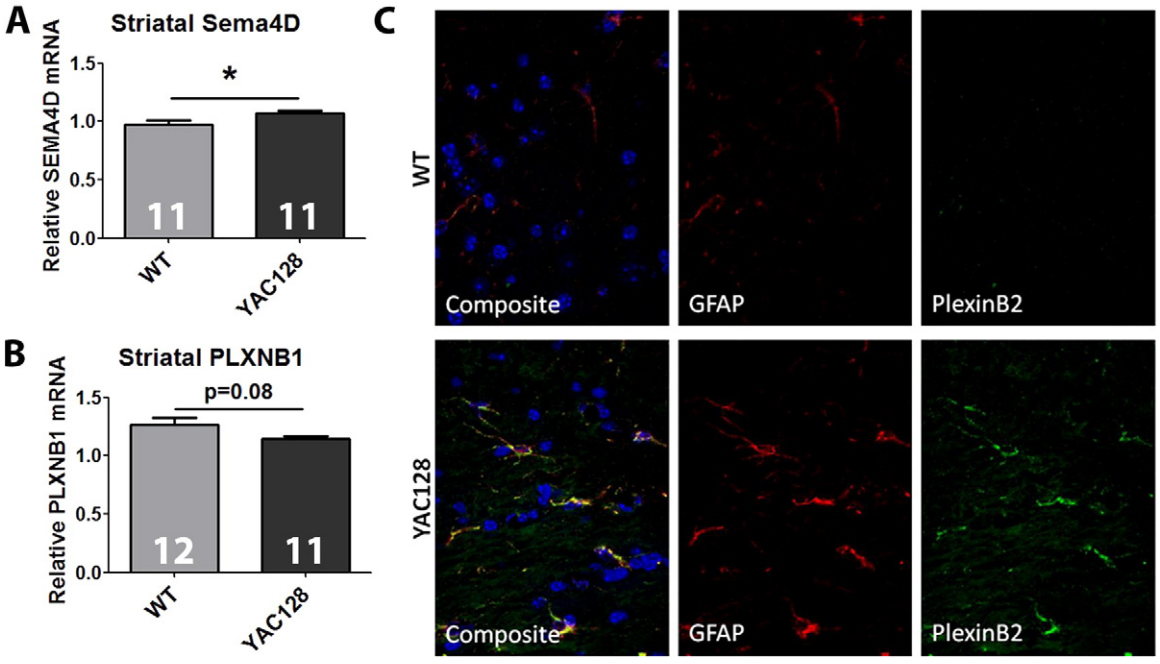

Fig. 1. The SEMA4D signaling pathway is dysregulated in YAC128 striatum. (A,B) qRT-PCR was used to measure the relative gene expression level of (A) SEMA4D and (B) Plexin-B1 in striatal lysates from 12 month-old YAC128 and WT mice. * = $p < .05$. (C) Sections from 12 month old YAC128 and WT brain were co-stained for plexin-B2 (PlexinB2, green) and astrocyte marker GFAP (red). Composite images with DAPI (blue) to visualize cellular nuclei, are shown in the left-most panels. Slides were imaged at 60× magnification using an EXi-Aqua-14 bit camera coupled to an Olympus I × 50 microscope.

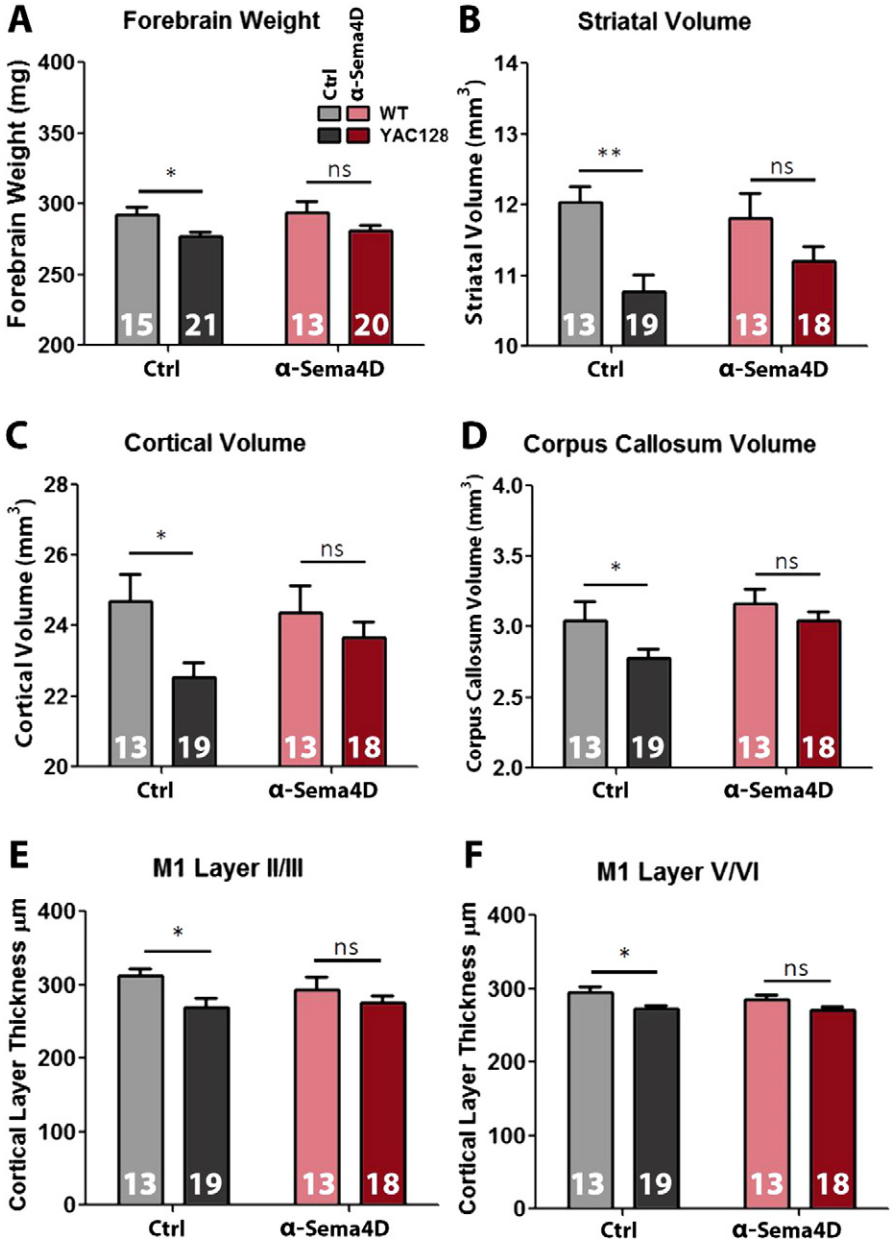

Fig. 2. Anti-SEMA4D treatment preserves brain gray and white matter. Neuropathology was evaluated at 12 months of age by (A) forebrain weight, (B) striatal volume, (C) cortical volume, (D) corpus callosum volume, and (E, F) cortical layer thickness in primary motor cortex. ns = not significant, * = $p < .05$, ** = $p < .01$.

a 5.4% reduction in forebrain weight (Fig. 2A), 10.4% striatal volume loss, and 8.7% cortical volume loss (Fig. 2B, C). An 8.8% reduction of corpus callosum volume, indicating loss of brain white matter, was also observed (Fig. 2D). Ctrl-treated YAC128 mice also displayed layer-specific thinning of primary motor cortex (Fig. 2E, F). Consistent with previous reports (Carroll et al., 2011b), there was no effect of genotype noted on cortical layer thickness in layers I or IV of primary motor cortex or in any layer of primary sensory cortex, and we observed no effect of α-Sema4D treatment in these regions (data not shown). α-Sema4D treatment ameliorated forebrain weight (4.3% loss), striatal volume (5.1% loss), cortical volume (2.9% loss), corpus callosum volume (3.8% loss), and thinning of cortical layers II/III and V/VI in YAC128 mice compared to Ctrl-treated YAC128 mice, indicating mAb-mediated inhibition of SEMA4D is broadly neuroprotective and capable of preserving both brain gray and white matter in the context of ongoing HD pathogenesis.

The integrated optical density (IOD) of DARPP-32 immunoreactivity was measured in a set of sections spaced 200 µM apart spanning the striatum. The IOD for each mouse was then normalized to the mean value for the WT Ctrl group from the same cohort. Ctrl-treated YAC128 mice displayed a trend toward reduced DARPP-32 immunoreactivity at 6 months of age and a significant 21.4% reduction at 12 months of age. This was improved by α-Sema4D treatment to a 5.6% reduction, a level that is not significantly different from α-Sema4D treated WT mice (Fig. 3). These treatment-specific volumetric changes, in aggregate, suggest inhibition of SEMA4D signaling impedes regional brain degeneration that progressively develops in the YAC128 HD mouse model.

Peripheral pathology

Levels of huntingtin are highest in the brain and testes (Strong et al., 1993), and while fertility is generally unaffected (Pridmore and Adams, 1991), men with HD exhibit reduced testosterone concentrations as well as marked testicular degeneration (Markianos et al., 2005; Van Raamsdonk et al., 2007). Consistent with previous reports (Van Raamsdonk et al., 2006; Van Raamsdonk et al., 2005),

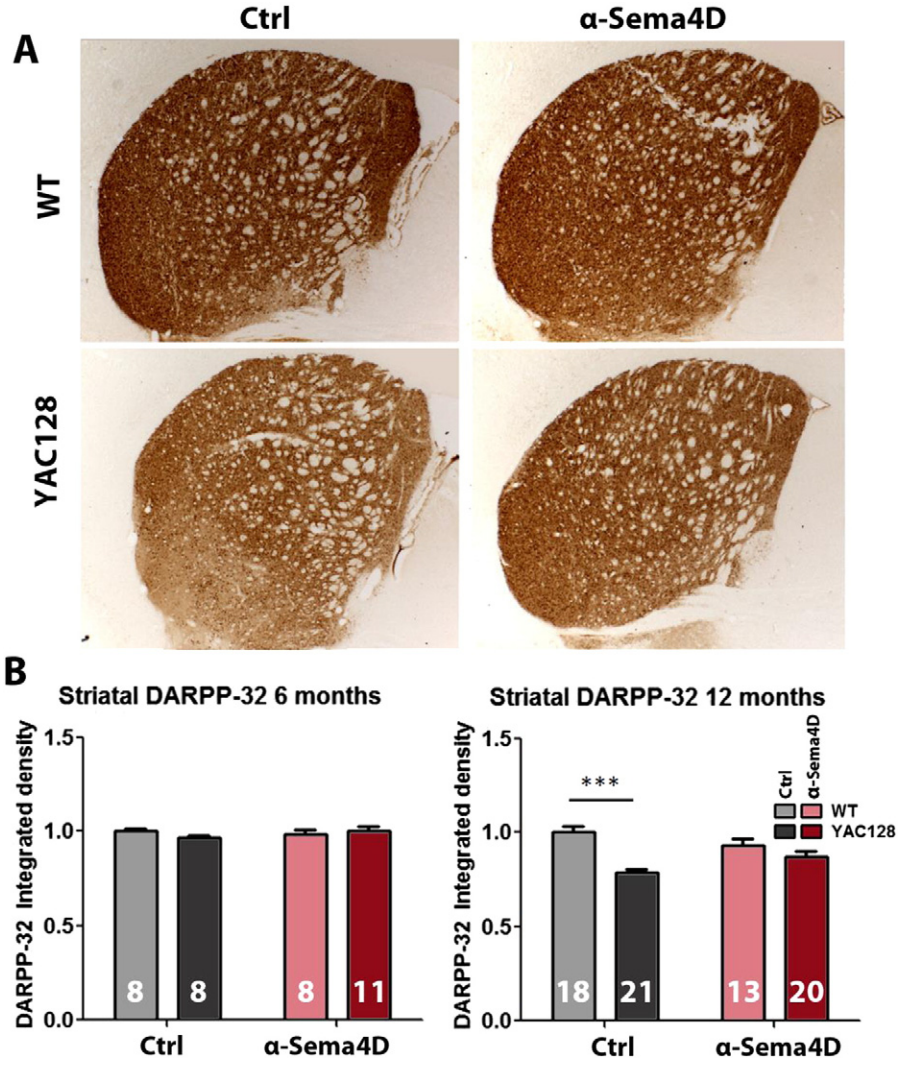

Fig. 3. Anti-SEMA4D treatment preserves striatal DARPP-32 expression. To evaluate health of striatal medium spiny neurons, DARPP-32 immunoreactivity was quantified at 6 and 12 months of age. (A) Representative images from 12 month-old animals. (B) Total integrated optical density normalized to mean WT Ctrl values from the same cohort. *** = $p < .001$.

at 12 months of age the testes of Ctrl-treated YAC128 mice were significantly smaller than those of Ctrl-treated WT mice, indicating testicular degeneration. This degeneration was completely prevented by α-Sema4D treatment, as testis weights were indistinguishable between WT and α-Sema4D treated YAC128 male mice (Fig. 4).

Fig. 4. Anti-SEMA4D treatment prevents testicular degeneration in YAC128 mice. Testis weight was assessed in post-perfusion 12 month-old male mice. Ctrl-treated YAC128 mice had smaller testis than WT mice, indicating testicular degeneration. Conversely, there was no loss of testis weight observed in α-Sema4D treated YAC128 mice, demonstrating rescue of the testicular degeneration phenotype. * = $p < .05$.

Another peripheral abnormality reported to affect nearly all individuals with HD and some other HD transgenic models, and which is not necessarily associated with pathology of the CNS, is progressive weight loss due to purported effects of muHTT expression on the digestive system and adipocyte function (Aziz et al., 2008; Phan et al., 2009). Conversely, full-length human HTT transgenic mouse models, including the YAC128, exhibit significant weight gain (Gray et al., 2008; Slow et al., 2003). This weight gain is modulated by levels of transgenic HTT (Van Raamsdonk et al., 2006), which is indicative of HTT-associated metabolic abnormalities, despite the inverse phenotype. Body weight of α-Sema4D or Ctrl-treated YAC128 and WT mice was compared at 2-month intervals from 2 to 12 months of age (Fig. S3). As expected, Ctrl-treated YAC128 mice, especially females, displayed an increase in body weight compared to Ctrl-treated WT mice. α-Sema4D treatment had no effect on the body weight of YAC128 mice.

Evaluation of α-Sema4D mAb67-2 levels in longitudinal serum

mAb67-2 concentration was measured in pooled sera at 3, 6, 9, and 12 months of age for all groups (Table S1). Sera from mAb67-2 treated animals contained expected levels of drug consistent with previous studies (Smith et al., 2014). However, mAb67-2 was also detected at much lower levels (25 to 25,000-fold less) in sera from both Ctrl-treated groups. When sera from each animal were evaluated

independently (data not shown), it was determined that mAb67-2 was detectable in nearly all the animals. Due to the global nature, this is likely the result of cross-contamination. α-Sema4D and Ctrl-treated animals were inter-housed during the study in order to ensure that the researchers performing the experiments remained blind to the treatment, and to eliminate any potential housing bias within the data. Inter-housed animals are in continual close contact and groom one another. If mAb67-2 leaks following IP immunization or is excreted from recipient animals in an active, non-metabolized form, and is cutaneously or orally bioavailable, inter-housing could result in low levels of drug in the Ctrl-treated cage mates of α-Sema4D treated animals. Despite the low levels of mAb67-2 detected in Ctrl-treated groups, the expected pathologic differences between Ctrl-treated YAC128 and WT mice were readily observed, indicating that the very low level of drug in these animals was below the threshold of activity.

Motor performance

To determine if anti-SEMA4D immunotherapy could alleviate the known motor deficits of YAC128 mice, treated mice underwent longitudinal rotarod and climbing testing (Fig. 5). Compared to Ctrl-treated WT mice, Ctrl-treated YAC128 mice displayed expected deficits, showing a progressive decline in rotarod performance and time spent climbing. Ctrl-treated YAC128 mice fell from the accelerating rotarod significantly sooner than WT mice from 4 months of age and onward. α-Sema4D treated YAC128 mice were not significantly different from Ctrl-treated WT mice until 6 months of age. However, they too exhibited declining rotarod performance that was indistinguishable from Ctrl-treated YAC128 mice (Fig. 5A). Both Ctrl and α-Sema4D treated YAC128 mice displayed progressive deficits in spontaneous climbing with an increased latency to begin climbing, decreased number of climbing events, and decreased time spent climbing as compared to Ctrl-treated WT mice (Fig. 5B–D). Taken together, these data indicate that anti-SEMA4D immunotherapy does not improve motor performance of YAC128 mice.

Cognitive performance

Prior to clinical diagnosis, individuals with HD begin to manifest modest cognitive deficits that primarily relate to erosion of procedural memory (the ability to learn and recall new motor skills) and visuospatial memory recall (Butters et al., 1985). To assess the effects of SEMA4D inhibition on cognitive function in YAC128 mice, mice were evaluated for motor learning during rotarod training at 2 months of age, for spontaneous alternation during exploration of a T maze at 4 months of age, and for object location and recognition learning at 6 months of age (Figs. 6 and S4). While both Ctrl and α-Sema4D treated YAC128 mice displayed increased falls and decreased latency to fall from the rotarod on day 1 of training, there was a trend toward reduced falls in the α-Sema4D treated group. On day 2 of training and on the test day, Ctrl-treated YAC128 mice displayed decreased latency to fall compared to Ctrl-treated WT mice, while at these time points, α-Sema4D treated YAC128 mice were not significantly different from WT Ctrl mice (Fig. 6A,B), indicating improved motor learning in α-Sema4D treated YAC128 mice. In another cognitive paradigm, α-Sema4D treatment rescued the object learning deficits of YAC128 mice. Ctrl and α-Sema4D treated WT mice displayed a preference for investigating a known object in a novel location, while Ctrl-treated YAC128 mice displayed no preference; investigating both the object in the original location and the object in the novel location equally. α-Sema4D treatment restored the preference for an object in a novel location in YAC128 mice (Fig. 5C), indicating a rescue of spatial learning deficits. In addition, both groups of WT mice displayed a preference for investigating a novel object over a known object, while Ctrl-treated YAC128 mice displayed no preference; investigating both the novel and known objects equally. α-Sema4D treatment restored the preference for a novel object in YAC128 mice, indicating a rescue of object recognition deficits.

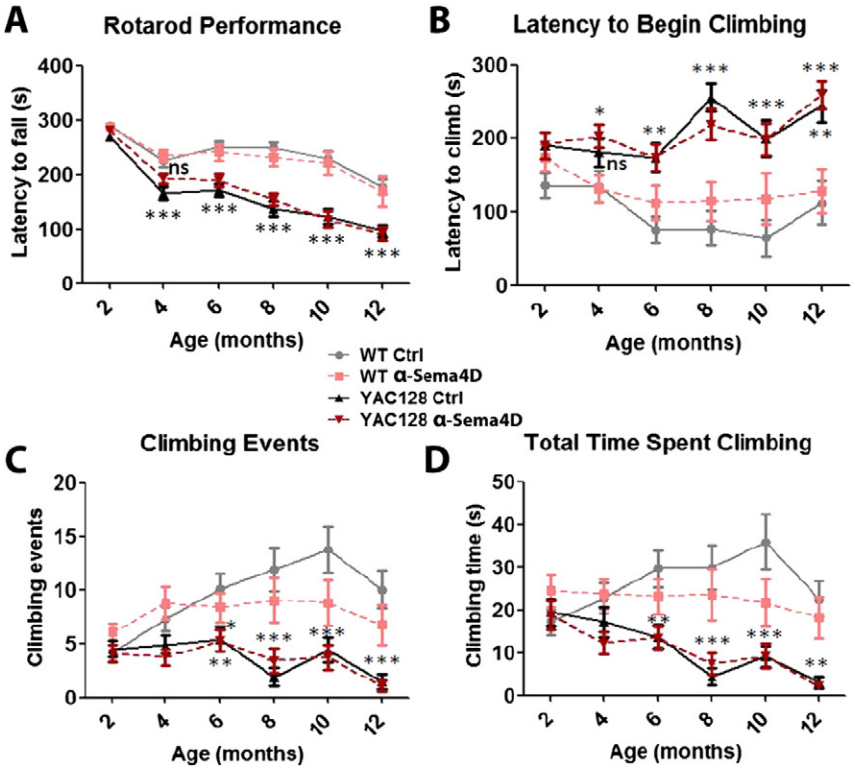

Fig. 5. Anti-SEMA4D treatment has no effect on motor deficits of YAC128 mice. Mice were assessed for motor performance by longitudinal accelerating rotarod (A) and spontaneous climbing (B–D) at 2 month intervals from 2 to 12 months of age. ns = not significant, * = $p < .05$, ** = $p < .01$, *** = $p < .001$.

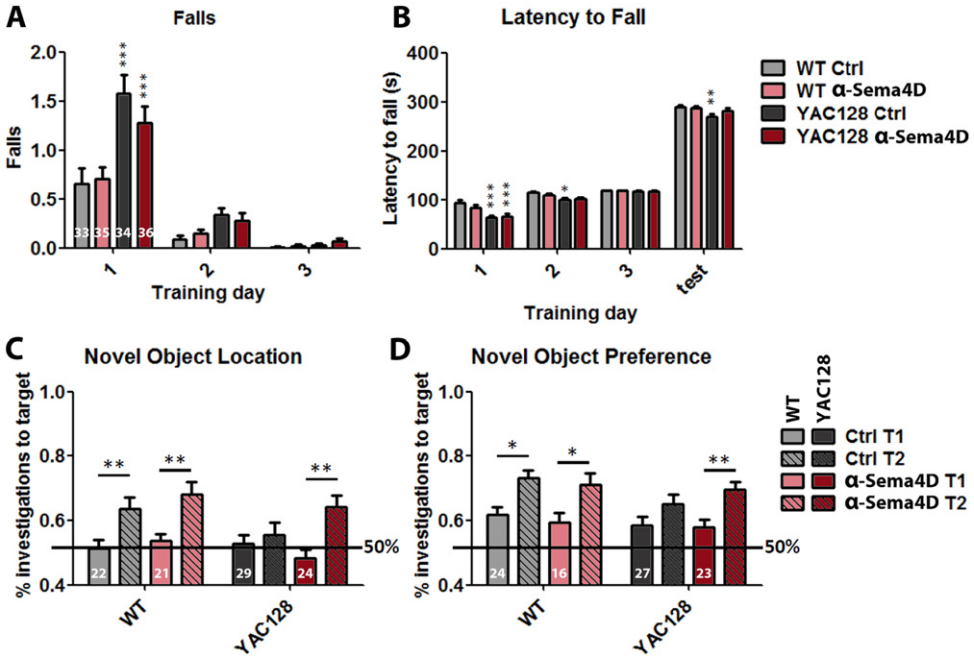

Fig. 6. Anti-SEMA4D treatment improves cognitive performance of YAC128 mice. Motor learning was evaluated at 2 months of age during three consecutive days of rotarod training (A, B). Spatial learning and object recognition were evaluated at 6 months of age by novel object location and novel object preference test, respectively (C, D). * = p < .05, ** = p < .01, *** = p < .001.

α-Sema4D treatment did not, however, have an effect on the spontaneous alternation deficit of YAC128 mice. Both Ctrl-treated and α-Sema4D treated YAC128 mice performed at roughly the level of chance in this assay, entering the previously explored and unexplored arms of the maze with equal frequency, while both WT groups preferentially entered the unexplored arm of the maze (Fig. S4).

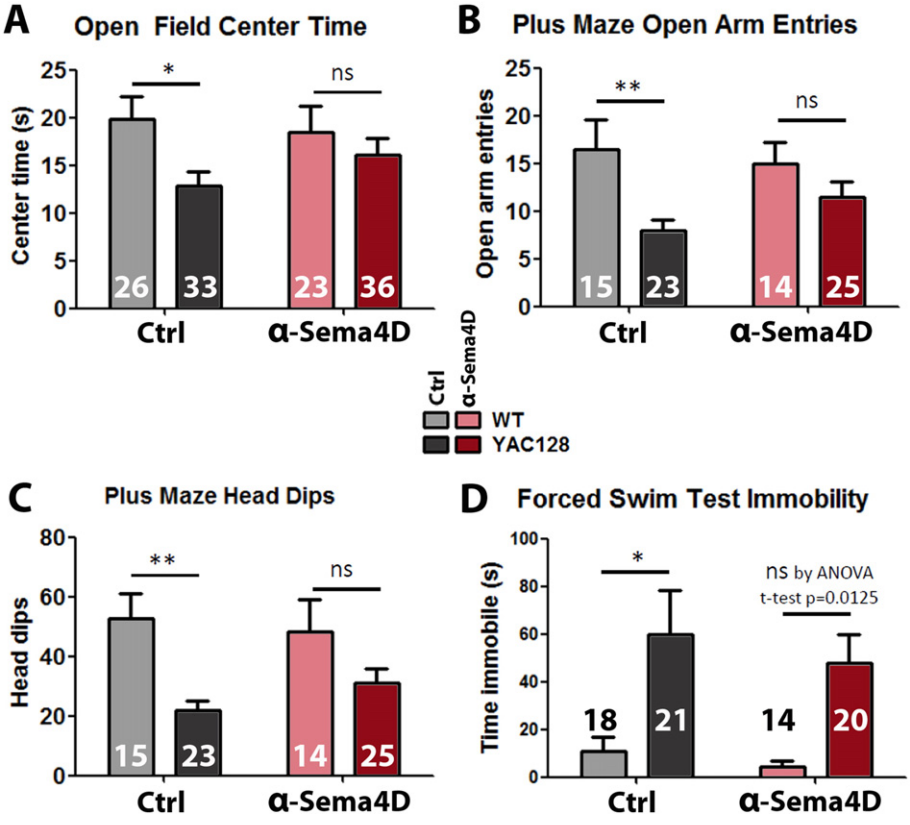

Fig. 7. Anti-SEMA4D treatment ameliorates anxiety-like behavior of YAC128 mice. To evaluate the effect of antibody-mediated SEMA4D blockade on psychiatric behaviors, Ctrl and α-Sema4D treated mice were evaluated for time spent in the center of an open field under bright lighting during a 10-min exploration at 6 months of age as a measure of anxiety (A), and for entries into the open arms and head dips off the side of the open arms of an elevated plus maze during a 5-min exploration at 8 months of age as a measure of anxiety (B, C), and for immobility during the last 5 minutes of a 6 minute forced swim at 12 months of age as a measure of depressive behavior (D). ns = not significant, * = p < .05, ** = p < .01.

Psychiatric behavior

Depression, irritability, and impulsivity are the most common psychiatric features exhibited by HD-afflicted individuals (Duff et al., 2007). These psychiatric behaviors typically present prior to full disease onset and negatively impact overall quality of life. To evaluate the effect of anti-SEMA4D immunotherapy on psychiatric-like phenotypes of YAC128 mice, treated mice were assessed at 6 months of age during open field exploration, at 8 months of age during elevated plus maze exploration, and at 12 months of age using a modified Porsolt forced swim test (Fig. 7). As compared to Ctrl-treated WT mice, Ctrl-treated YAC128 mice displayed expected anxiety-like phenotypes, spending significantly less time in the center of the open field and less frequently entering into or dipping their heads off of the edge of the open arms of the elevated plus maze. While no significant effects of α-Sema4D treatment were observed in these measures, treatment did induce a trend toward increased center time, open arm entries, and head dips in YAC128 mice resulting in no significant differences between α-Sema4D treated WT and YAC128 mice (Fig. 7A–C), suggesting a benefit to anxiety-like behavior. No effects of genotype or treatment were observed on distance traveled or mean velocity during exploration of the open field or the elevated plus maze (Fig. S5), indicating that the differences observed in anxiety-like behavior were not the result of altered spontaneous exploratory activity. In a separate test of depressive-like behavior, Ctrl-treated YAC128 mice spent significantly more time immobile and less time swimming than Ctrl-treated WT mice during forced swimming. However, while no significant difference in depressive-like behavior was observed between α-Sema4D treated WT and YAC128 mice by 2-way-ANOVA, the genotypic difference remained quite large in treated mice, and a binary *t*-test of only the α-Sema4D treated groups was significant ($p = 0.0125$), suggesting that depressive-like behavior persists in these animals.

Discussion

Anti-semaphorin 4D immunotherapy provided significant benefit to the HD-like neuropathological and behavioral phenotypes of the YAC128 transgenic mouse model of HD. In many cases the effect of α-Sema4D treatment was greater in YAC128 than in WT mice or only apparent in YAC128 mice, indicating modification of HD-related pathogenic processes. In particular, SEMA4D blockade improved several HD-related pathologies including testicular degeneration and striatal, cortical, and corpus callosum volume loss as well as improving a subset of learning deficits and anxiety-like behavior.

α-Sema4D treatment significantly increased corpus callosum volume in both genotypes. This is consistent with previous reports that SEMA4D inhibition increases proliferation, maturation, and migration oligodendrocyte precursor cells (Smith et al., 2014). The increase in corpus callosum volume following α-Sema4D treatment was more pronounced in YAC128 than WT mice and resulted in amelioration of the atrophy phenotype. Additionally, in all stereological measurements evaluated there were no significant differences observed between anti-SEMA4D treated WT and YAC128 animals while in most instances significant differences were observed between Ctrl-treated WT and YAC128 animals. The striking lack of difference between the α-Sema4D treated WT and YAC128 groups in these broad measures indicates that anti-SEMA4D treatment promotes preservation of both brain gray and white matter, outcomes with profound therapeutic potential.

Anti-SEMA4D immunotherapy fully rescued testicular degeneration in YAC128 males. The HTT protein is expressed ubiquitously, however, expression is by far the highest in the brain and testes (Sharp et al., 1995). The mechanisms leading to testicular degeneration in HD are thought to include intrinsic apoptotic death of spermatogenic and Sertoli cells mediated by muHTT (Leavitt et al., 2001). SEMA4D is expressed in the testes (Hall et al., 1996), and our data indicate that it may play a role in muHTT-induced testicular cell death similar to its role in death of immature neurons and oligodendrocytes in the brain. In fact, there is significant similarity in the role of SEMA4D in actin networks and vesicle transport in the nervous system (Kuzirian et al., 2013), and the HTT protein, which, in one of its many roles, is a cytoskeletal scaffold that mediates vesicular and molecular transport (Caviston and Holzbaur, 2009; Caviston et al., 2011). The muHTT protein perturbs this process, potentially leading to initiation of SEMA4D-mediated cytoskeletal breakdown and subsequent apoptosis, which may be prevented by anti-SEMA4D mAb-based treatment.

Anti-SEMA4D immunotherapy did not provide benefit to the motor deficits in YAC128 mice. However, HD patients commonly report that it is the cognitive and psychiatric aspects of the disease that most negatively impact their quality of life (Adam and Jankovic, 2008), and these aspects of the YAC128 HD-like phenotype were improved by SEMA4D blockade. Benefits to psychiatric aspects were apparent in amelioration of anxiety-like behavior in both the open field and elevated plus maze exploration tasks. The effect of α-Sema4D administration on cognitive performance was mixed. A small improvement to motor learning during rotarod training was observed at two months of age. It is possible that treatment related changes would increase with age, however, as motor deficits were not improved, a full rescue of the motor learning deficit might not be expected even given a complete recovery of cognitive performance. There was no effect of α-Sema4D on the spontaneous alternation deficit of YAC128 mice, indicating that treated mice still had spatial learning deficits. However, anti-SEMA4D treatment resulted in a full rescue of object location spatial learning. As the spontaneous alternation task is carried out in a completely symmetrical and unmarked T maze, it is likely a more difficult spatial discrimination task than the object location task, which is asymmetrical (Southwell et al., 2009). Supporting this is the finding that spontaneous alternation deficits are apparent in YAC128 mice prior to the onset of object location learning deficits (unpublished observation). The differential difficulty of these two tasks could account for rescue being observed in one paradigm but not the other. α-Sema4D administration also resulted in a complete rescue of the object recognition deficits of YAC128 mice. Taken together, these data indicate that the psychiatric and cognitive aspects of the HD-like phenotypes of YAC128 mice are improved, but not abolished by anti-SEMA4D mAb treatment.

Striatal medium spiny neurons (MSNs) play a pivotal role in motor control (reviewed by Graybiel et al., 1994). MSNs receive significant dopaminergic and glutamatergic input via the substantia nigra pars compacta and cortex, respectively, and their function and viability are believed to be especially susceptible in the setting of HD due to multiple intrinsic and extrinsic mechanisms (reviewed by Ehrlich, 2012). Intrinsic processes that have been shown to underlie HD-related MSN dysfunction and eventual demise include abnormal aggregation and clearance of polyQ-htt, mitochondrial dysfunction, diminished neurotrophin levels, transcriptional dysregulation, disruption of axonal transport, and excitotoxicity, while extrinsic mechanisms include astrocyte and oligodendrocyte dysfunction, microglial activation, and abnormal cortical neuron function (Ehrlich, 2012; Zuccato et al., 2010). While striatal volume (Fig. 1) and DARPP-32 expression (Fig. 2) within the striatum were relatively preserved by anti-SEMA4D treatment, the inability of anti-SEMA4D immunotherapy to improve motor function in YAC128 mice may reflect persistent functional deficits related to the inherent susceptibility of MSNs to intrinsic pathogenic mechanisms, which represent cellular processes that currently are not known to be overtly regulated by SEMA4D-Plexin signaling.

The blood–brain barrier (BBB) in the setting of HD pathogenesis is not generally thought to be significantly compromised, especially when compared to the highly damaged neurovascular unit in other neuroinflammatory/neurodegenerative diseases, such as MS and AD (reviewed by Neuwelt et al., 2011). For example, comparison of BBB permeability values between the aggressive R6/2 model of HD and wild-type littermates revealed no significant differences (Cepeda-

Prado et al., 2012). Interestingly, however, Lin et al. recently reported that R6/2 mice as well as humans with HD exhibit detectable enhancements in microvasculature densities (Lin et al., 2013), and progressive neurovascular abnormalities have previously been reported in YAC128 mice (Franciosi et al., 2012), which suggests some degree of disease-related dysfunction in the HD neurovascular unit. As reported elsewhere, SEMA4D blocking antibody preserves the integrity of the BBB under inflammatory conditions by preventing downregulation of Claudin-5 and breakdown of endothelial tight junctions (Smith et al., 2014). It is possible that this also contributes to therapeutic benefit in HD.

Despite the pleiotropic effects of treatment with anti-SEMA4D antibody, modulating BBB integrity, promoting neuronal process extension, and oligodendrocyte differentiation/viability, we did not observe any drug-related side effects/toxicities of anti-SEMA4D antibody in this study. Moreover, single and 6 month repeat-dose toxicity, pharmacokinetic, and pharmacodynamic studies with a humanized, mAb67-2-derived anti-SEMA4D IgG4 antibody (VX15/2503) have been completed in cynomolgus monkeys and rats at doses up to 200 mg/kg with no toxicity observed (manuscript in preparation). VX15/2503 has completed a Phase I clinical trial in patients with solid tumors (clinicaltrials.gov identifier: NCT01313065) and is currently enrolling patients in the highest dose cohort of a phase 1 trial in patients with multiple sclerosis (clinical trials.gov identifier: NCT01764737) in support of safety and tolerability of VX15/2503 in these patient populations. Given its highly relevant mechanisms of action, with further validation, and possibly in combination with other drug(s), such as tetrabenazine, which can moderate motor symptoms (Group, 2006), mAb-based SEMA4D inhibition could serve as a much needed disease-modifying therapy for HD.

Additionally this work further demonstrates the similarity of pathogenic mechanisms in neuroinflammatory and neurodegenerative diseases and provides rationale for the re-purposing of therapeutics developed for other such indications in the treatment of HD.

Acknowledgments

The authors thank Garnet Martens and the University of British Columbia Bioimaging Facility for assistance with optical density quantitation, Mahsa Amirabassi and Mark Wang for excellent animal care, and Qingwen Xia for assistance with genotyping.

Conflicts of interest statement

L.A.W., J.V., and A.J., E.S.S., W.J.B., and M.Z. are employees of, with a financial interest in, Vaccinex Inc. This work in the laboratory of Dr. Michael Hayden was supported by Vaccinex Inc. Employees of Vaccinex Inc. contributed to the study design, performed quantitation of mAb67-2 in animal sera, and participated in the revision of the report. Vaccinex Inc. played no role in animal treatment, testing, or collection, nor analysis of data and interpretation of results. M.R.H. is an employee of Teva Pharmaceuticals. Teva Pharmaceuticals played no role in this study.

Appendix A. Supplementary data

Supplementary data to this article can be found online at http://dx.doi.org/10.1016/j.nbd.2015.01.002.

References

Adam, O., Jankovic, J., 2008. Symptomatic treatment of Huntington disease. Neurotherapeutics 5, 181–197.
Aziz, N., et al., 2008. Weight loss in Huntington disease increases with higher CAG repeat number. Neurology 71, 1506–1513.
Becanovic, K., et al., 2010. Transcriptional changes in Huntington disease identified using genome-wide expression profiling and cross-platform analysis. Hum. Mol. Genet. 19, 1438–1452.
Bjorkqvist, M., et al., 2008. A novel pathogenic pathway of immune activation detectable before clinical onset in Huntington's disease. J. Exp. Med. 205, 1869–1877.
Borjabad, A., Volsky, D., 2012. Common transcriptional signatures in brain tissue from patients with HIV-associated neurocognitive disorders, Alzheimer's disease, and multiple sclerosis. J. Neuroimmune Pharmacol. 7, 914–926.
Bougeret, C., et al., 1992. Increased surface expression of a newly identified 150-kDa dimer early after human T lymphocyte activation. J. Immunol. 148, 318–323.
Butters, N., et al., 1985. Memory disorders associated with Huntington's disease: verbal recall, verbal recognition and procedural memory. Neuropsychologia 23, 729–743.
Carroll, J., et al., 2011a. Mice lacking caspase-2 are protected from behavioral changes, but not pathology, in the YAC128 model of Huntington disease. Mol. Neurodegener. 6, 59.
Carroll, J.B., et al., 2011b. Natural history of disease in the YAC128 mouse reveals a discrete signature of pathology in Huntington disease. Neurobiol. Dis. 43, 257–265.
Caviston, J.P., Holzbaur, E.L.F., 2009. Huntingtin as an essential integrator of intracellular vesicular trafficking. Trends Cell Biol. 19, 147–155.
Caviston, J.P., et al., 2011. Huntingtin coordinates the dynein-mediated dynamic positioning of endosomes and lysosomes. Mol. Biol. Cell 22, 478–492.
Cepeda-Prado, E., et al., 2012. R6/2 Huntington's disease mice develop early and progressive abnormal brain metabolism and seizures. J. Neurosci. 32, 6456–6467.
Duff, K., et al., 2007. Psychiatric symptoms in Huntington's disease before diagnosis: the predict-HD study. Biol. Psychiatry 62, 1341–1346.
Ehrlich, M., 2012. Huntington's disease and the striatal medium spiny neuron: cell-autonomous and non-cell-autonomous mechanisms of disease. Neurotherapeutics 9, 270–284.
Ehrnhoefer, D.E., et al., 2011. Convergent pathogenic pathways in Alzheimer's and Huntington's diseases: shared targets for drug development. Nat. Rev. Drug Discov. 10, 853–867.
Elhabazi, A., et al., 2001. Biological activity of soluble CD100. I. The extracellular region of CD100 is released from the surface of T lymphocytes by regulated proteolysis. J. Immunol. 166, 4341–4347.
Ellwardt, E., Zipp, F., 2014. Molecular mechanisms linking neuroinflammation and neurodegeneration in MS. Exp. Neurol. 262, Pt A:8–17.
Ernst, A., et al., 2014. Neurogenesis in the striatum of the adult human brain. Cell 156, 1072–1083.
Franciosi, S., et al., 2012. Age-dependent neurovascular abnormalities and altered microglial morphology in the YAC128 mouse model of Huntington disease. Neurobiol. Dis. 45, 438–449.
Furuyama, T., et al., 1996. Identification of a novel transmembrane semaphorin expressed on lymphocytes. J. Biol. Chem. 271, 33376–33381.
Giraudon, P., et al., 2004. Semaphorin CD100 from activated T lymphocytes induces process extension collapse in oligodendrocytes and death of immature neural cells. J. Immunol. 172, 1246–1255.
Gray, M., et al., 2008. Full-length human mutant huntingtin with a stable polyglutamine repeat can elicit progressive and selective neuropathogenesis in BACHD mice. J. Neurosci. 28, 6182–6195.
Graybiel, A.M., et al., 1994. The basal ganglia and adaptive motor control. Science 265, 1826–1831.
Group, H.S., 2006. Tetrabenazine as antichorea therapy in Huntington disease: a randomized controlled trial. Neurology 66.
Hall, K.T., et al., 1996. Human CD100, a novel leukocyte semaphorin that promotes B-cell aggregation and differentiation. Proc. Natl. Acad. Sci. 93, 11780–11785.
HDCRG, 1993. A novel gene containing a trinucleotide repeat that is expanded and unstable on Huntington's disease chromosomes. The Huntington's Disease Collaborative Research Group. Cell 72, 971–983.
Hodges, A., et al., 2006. Regional and cellular gene expression changes in human Huntington's disease brain. Hum. Mol. Genet. 15, 965–977.
Hota, P., Buck, M., 2012. Plexin structures are coming: opportunities for multilevel investigations of semaphorin guidance receptors, their cell signaling mechanisms, and functions. Cell. Mol. Life Sci. 69, 3765–3805.
Kuhn, A., et al., 2007. Mutant huntingtin's effects on striatal gene expression in mice recapitulate changes observed in human Huntington's disease brain and do not differ with mutant huntingtin length or wild-type huntingtin dosage. Hum. Mol. Genet. 16, 1845–1861.
Kumanogoh, A., et al., 2000. Identification of CD72 as a lymphocyte receptor for the class IV semaphorin CD100: a novel mechanism for regulating B cell signaling. Immunity 13, 621–631.
Kuzirian, M.S., et al., 2013. The class 4 semaphorin Sema4D promotes the rapid assembly of GABAergic synapses in rodent hippocampus. J. Neurosci. 33, 8961–8973.
Lassmann, H., 2011. Mechanisms of neurodegeneration shared between multiple sclerosis and Alzheimer's disease. J. Neural Transm. 118, 747–752.
Leavitt, B.R., et al., 2001. Wild-type huntingtin reduces the cellular toxicity of mutant huntingtin in vivo. Am. J. Hum. Genet. 68, 313.
Lin, C.-Y., et al., 2013. Neurovascular abnormalities in humans and mice with Huntington's disease. Exp. Neurol. 250, 20–30.
Markianos, M., et al., 2005. Plasma testosterone in male patients with Huntington's disease: relations to severity of illness and dementia. Ann. Neurol. 57, 520–525.
Neuwelt, E.A., et al., 2011. Engaging neuroscience to advance translational research in brain barrier biology. Nat. Rev. Neurosci. 12, 169–182.
Okuno, T., et al., 2010. Roles of Sema4D-plexin-B1 interactions in the central nervous system for pathogenesis of experimental autoimmune encephalomyelitis. J. Immunol. 184, 1499–1506.

Paradis, S., et al., 2007. An RNAi-based approach identifies molecules required for glutamatergic and GABAergic synapse development. Neuron 53, 217–232.
Phan, J., et al., 2009. Adipose tissue dysfunction tracks disease progression in two Huntington's disease mouse models. Hum. Mol. Genet. 18, 1006–1016.
Pouladi, M.A., et al., 2009. Prevention of depressive behaviour in the YAC128 mouse model of Huntington disease by mutation at residue 586 of huntingtin. Brain 132, 919–932.
Pridmore, S.A., Adams, G.C., 1991. The fertility of HD-affected individuals in Tasmania. Aust. N. Z. J. Psychiatry 25, 262–264.
Raissi, A.J., et al., 2013. Sema4D localizes to synapses and regulates GABAergic synapse development as a membrane-bound molecule in the mammalian hippocampus. Mol. Cell. Neurosci. 57, 23–32.
Ross, C.A., Tabrizi, S.J., 2011. Huntington's disease: from molecular pathogenesis to clinical treatment. Lancet Neurol. 10, 83–98.
Sharp, A.H., et al., 1995. Widespread expression of Huntington's disease gene (IT15) protein product. Neuron 14, 1065–1074.
Shi, W., et al., 2000. The class IV semaphorin CD100 plays nonredundant roles in the immune system: defective B and T Cell activation in CD100-deficient mice. Immunity 13, 633–642.
Slow, E.J., et al., 2003. Selective striatal neuronal loss in a YAC128 mouse model of Huntington disease. Hum. Mol. Genet. 12, 1555–1567.
Smith, E.S., et al., 2014. SEMA4D compromises Blood–Brain Barrier and inhibits remyelination in neurodegenerative disease. Neurobiol. Dis. 73C, 254–268.
Southwell, A.L., et al., 2009. Intrabody gene therapy ameliorates motor, cognitive, and neuropathological symptoms in multiple mouse models of Huntington's disease. J. Neurosci. 29, 13589–13602.
Southwell, A.L., et al., 2013. A fully humanized transgenic mouse model of Huntington disease. Hum. Mol. Genet. 22, 18–34.
Strong, T.V., et al., 1993. Widespread expression of the human and rat Huntington's disease gene in brain and nonneural tissues. Nat. Genet. 5, 259–265.
Suzuki, K., et al., 2008. Semaphorins and their receptors in immune cell interactions. Nat. Immunol. 9, 17–23.
Swiercz, J.M., et al., 2002. Plexin-B1 directly interacts with PDZ-RhoGEF/LARG to regulate RhoA and growth cone morphology. Neuron 35, 51–63.
Tabrizi, S.J., et al., 2009. Biological and clinical manifestations of Huntington's disease in the longitudinal TRACK-HD study: cross-sectional analysis of baseline data. Lancet Neurol. 8, 791–801.
Van Raamsdonk, J.M., et al., 2005. Loss of wild-type huntingtin influences motor dysfunction and survival in the YAC128 mouse model of Huntington disease. Hum. Mol. Genet. 14, 1379–1392.
Van Raamsdonk, J.M., et al., 2006. Body weight is modulated by levels of full-length Huntingtin. Hum. Mol. Genet. 15, 1513–1523.
Van Raamsdonk, J.M., et al., 2007. Testicular degeneration in Huntington disease. Neurobiol. Dis. 26, 512–520.
Yamaguchi, W., et al., 2012. Sema4D as an inhibitory regulator in oligodendrocyte development. Mol. Cell. Neurosci. 49, 290–299.
Yang, Y.-H., et al., 2011. Plexin-B1 activates NF-kB and IL-8 to promote a pro-angiogenic response in endothelial cells. PLoS One 6, e25826.
Zhu, L., et al., 2007. Regulated surface expression and shedding support a dual role for semaphorin 4D in platelet responses to vascular injury. Proc. Natl. Acad. Sci. 104, 1621–1626.
Zuccato, C., et al., 2010. Molecular mechanisms and potential therapeutical targets in Huntington's disease. Physiol. Rev. 90, 905–981.